Journal of Hazardous Materials 182 (2010) 266–272

Contents lists available at ScienceDirect

Journal of Hazardous Materials

journal homepage: www.elsevier.com/locate/jhazmat

Influence of the pH on the accumulation of phosphate by red mud (a bauxite ore processing waste)

Paola Castaldi*, Margherita Silvetti, Giovanni Garau, Salvatore Deiana

Dipartimento di Scienze Ambientali Agrarie e Biotecnologie Agro-Alimentari, University of Sassari, Viale Italia 39, 07100 Sassari, Italy

ARTICLE INFO

Article history:
Received 3 February 2010
Received in revised form 3 May 2010
Accepted 8 June 2010
Available online 15 June 2010

Keywords:
Red mud
Phosphate
Adsorption isotherms
Sequential extraction
FT-IR spectroscopy

ABSTRACT

In the present work we investigated the interactions established between red mud (RM) and phosphate anions (P) at pH 4.0, 7.0 and 10.0.

The amount of P sorbed by RM (P-RM) increased as the pH decreased being equal to 4.871 mmol g^{-1} at pH 4.0, 0.924 mmol g^{-1} at pH 7.0, and 0.266 mmol g^{-1} at pH 10.0. Sequential extractions' data of P-RM equilibrated at pH 4.0 and 7.0, suggested that the phosphate sorption at these pH values was mainly regulated by two different mechanisms that gave rise to a chemical adsorption on RM phases, and to the formation of metal phosphate precipitates. By contrast, at pH 10.0 the P-sorption was regulated by a chemisorption mechanism on Fe–Al phases of RM.

These findings were supported by FT-IR analysis, which showed a broad band at 1114 and 1105 cm^{-1} in P-RM spectra at pH 4.0 and 7.0 respectively, attributable to P–O(H) stretching ν_3-modes associated to inner-sphere complexes of phosphate on Fe–Al phases, or alternatively to stretching vibrations of PO_4^{3-} tetrahedra, arising from a precipitate of aluminium phosphate. Importantly, the FT-IR spectroscopy showed a phosphate-promoted dissolution of tectosilicates, notably cancrinite and sodalite, in RM exchanged with phosphate at pH 4.0 and 7.0.

1. Introduction

Phosphate is a soil element essential for plant growth, a macronutrient present in most of biological tissues, and has been recognized as one of the main nutrients limiting the growth of photosynthetic algae and other organisms living in surface water bodies [1–4]. However, an excessive presence of phosphate in wastewater is one of the main causes of eutrophication that affects many natural water bodies [2,4]. Therefore, its transport and fate in soils and aquifers, as well as its affinity towards soil colloids must be well understood to better evaluate its environmental impact. It is well known that mobility of phosphate anions in the environment is markedly influenced by mineral surfaces [3,5]. The phosphate anions strongly interact with iron and aluminium (hydr)oxides, which are important constituents of soils and sediments and key solids governing the transport and bioavailability of this and other anions [1,3]. The affinity of phosphate for (hydr)oxide surfaces depends on the complexing capacity of these latter, which allows binding of phosphate to surface groups by ligand-exchange reactions, and on the other hand on attractive or repulsive electrostatic interactions with the charged (hydr)oxide surfaces.

Recently, different types of low-cost sorbents, such as Fe/Al/Mn oxides and oxyhydroxides [1,3,6] zeolite and kaolinite [7,8], and untreated, acid and heat treated red muds (i.e. [2,4,9–11]) have been used for phosphate removal from polluted waters. Red muds, which are industrial wastes that remain after the digestion of bauxite during the Bayer process, are expected to be particularly effective in the removal and immobilization of both toxic anions and cations from wastewaters and polluted soils [11–14], thank to the combined presence of ferric, aluminium and tectosilicate-like compounds.

However, most of the studies that investigated the phosphate removal capacity of untreated or modified red muds (i.e. [2,4,9–11]) only considered the possible interaction mechanisms regulating the phosphate sorption by red mud (RM), while a much deeper knowledge would be essential in order to evaluate the red mud suitability over time as phosphate sorbent. Such a deeper knowledge could, for example, be provided by spectroscopic studies [10]. These could possibly provide useful details about the main phases of red mud that represent the active sites involved in the process of phosphate sorption, and could help elucidating the interaction mechanisms involved between phosphate and RM (e.g. chemical sorption, precipitation, and/or diffusion).

In a previous study we investigated the interaction mechanisms that regulate the accumulation and mobility of arsenate sorbed into RM and the mineralogical phases of RM actively involved in the

* Corresponding author. Tel.: +39 079229214; fax: +39 079229276.
E-mail address: castaldi@uniss.it (P. Castaldi).

0304-3894/$ – see front matter © 2010 Elsevier B.V. All rights reserved.
doi:10.1016/j.jhazmat.2010.06.025

Table 1
Properties of the RM_{nt} and RM samples at pH 10.0, 7.0 and 4.0 used in the study.

Chemical parameters	RM_{nt}	RM pH 10.0	RM pH 7.0	RM pH 4.0
pH	11.1	10.0	7.0	4.0
EC ($mS\,cm^{-1}$)	8.70	8.25	6.55	5.22
S_{BET}	19.5	21.4	23.6	25.5
PZC	4.77	–	–	–
Element composition (wt.%)				
C	9.15	9.00	9.32	n.d.
O	35.12	34.23	34.15	42.33
Na	5.17	4.31	2.30	1.15
Al	9.65	10.25	10.44	9.33
Si	4.32	4.94	4.53	3.41
Ca	1.04	1.13	1.15	1.00
Fe	30.35	30.88	32.53	35.32
Ti	4.13	4.23	4.53	6.43
Cl	1.07	1.03	1.05	1.03
Crystalline phases (wt.%)				
Cancrinite [$Na_6Ca_{1.5}Al_6Si_6O_{24}(CO_3)_{1.6}$]	4.0	4.0	3.5	n.d.
Sodalite [$Na_8(Cl,OH)_2|Al_6Si_6O_{24}$]	20.0	24.0	24.0	22.0
Hematite [Fe_2O_3]	44.0	42.0	42.0	49.0
Boehmite [AlO(OH)]	12.0	12.0	12.0	8.0
Gibbsite [$Al(OH)_3$]	4.0	4.0	4.0	4.0
Anatase [TiO_2]	4.5	4.0	4.0	5.5
Andradite [Ca–Fe–Al–Si oxide]	5.5	5.0	5.0	5.5
Quartz [SiO_2]	6.0	5.0	5.5	6.0

arsenate sorption [15]. The results obtained showed that sorption properties of the RM were significantly influenced by the pH, which affected the surface charge of the solid particles and the degree of ionization and speciation of arsenate species. The arsenate sorption in RM samples increased as the pH decreased (from 10.0 to 4.0), and the oxides/oxyhydroxides of Fe and Al (hematite, boehmite and gibbsite) of RM were the mineralogical phases involved in the sorption processes of arsenate [15]. In this study, we have considered the interaction mechanisms that control the sorption of phosphate into red mud, in order to better understand the affinity of red mud towards this anion, and the role of phosphate in arsenic polluted soils and waters, treated with red mud. The aim of this work is therefore (i) to assess, through adsorption isotherms performed under different pH conditions (pH 4.0, 7.0 and 10.0), the capacity of RM to interact with phosphate; (ii) to investigate, through a sequential extraction procedure, the interaction mechanisms that regulate the accumulation and mobility of phosphate by RM; and (iii) to determine, through Fourier transform infrared spectroscopy (FT-IR), the mineralogical phases of RM actively involved in the phosphate sorption and the types of surface complexes formed through the sorption of phosphate onto RM.

2. Materials and methods

2.1. Sample description

Red muds were obtained from the Eurallumina plant (Portovesme, Sardinia, Italy). The red muds were dried overnight at 105 °C, finely ground and sieved to <0.02 mm (RM_{nt}). The pH and electric conductivity (EC) values were determined in 1:2.5 ratio of red mud/distilled water (Table 1). The specific surface area of the RM_{nt} was determined by applying the BET model to the N_2 adsorption results obtained from a Sorptomatic Carlo Erba (Milan, Italy). The details on the sample pre-treatment are reported in Castaldi et al. [15].

The element composition of RM_{nt} and RM at pH 4.0, 7.0 and 10.0 was analyzed using Energy Dispersive X-ray (EDX) by JOEL model JSM-6480LV (Table 1). X-ray diffraction (XRD) analysis of RM_{nt} and RM at pH 4.0, 7.0 and 10.0 was carried out with a Rigaku D/MAX diffractometer (Cu Kα) equipped with a graphite monochromator in the diffracted beam (Table 1). The pattern was collected in the 2θ range from 10° to 70°. Aside from crystalline phases, about the 20 wt.% of the red mud samples was made of amorphous oxides. A more detailed description of crystalline phases identification is reported in Castaldi et al. [16].

2.2. Adsorption isotherms of phosphate on RM at pH 4.0, 7.0 and 10.0

All chemicals were of analytical grade and used without further purification. Red mud samples were artificially enriched with solutions containing increasing concentrations of $NaH_2PO_4{\cdot}7H_2O$ to obtain adsorption isotherms. Three batch experiments were prepared at three pH values (4.0, 7.0 and 10.0) and at constant temperature (25 ± 1 °C). Polyethylene bottles containing 1.0 g of red mud were filled with 25 mL of phosphate enriched solutions. Particularly 14 points on the whole were obtained to create the adsorption isotherm, corresponding to the addition of different volume of a 0.4 M $NaH_2PO_4{\cdot}7H_2O$ solution. The concentration of $NaH_2PO_4{\cdot}7H_2O$ added to 1.0 g of red muds varied between 4×10^{-4} and 0.40 M (which correspond to 0.01 and 10.0 mmol 25 mL^{-1} respectively). A background electrolyte of 0.1 M NaCl was used as diluent for all batch experiments. The pH values (4.0, 7.0, and 10.0) of the red mud not-exchanged and of the mixtures RM/polluting solution were adjusted with either 0.01, 0.1 or 1.0 M HCl or NaOH solutions. The mixtures (1:25 ratio of red mud/phosphate solution) were shaken for 24 h at constant temperature (25 ± 1 °C). Preliminary kinetic tests confirmed that this time was sufficient to reach the equilibrium (data not shown). After equilibrium, the samples were centrifuged at 8000 rpm for 10 min and filtered to completely separate the liquid and solid phases. An aliquot of the supernatant was taken and analyzed. P was measured by ionic chromatography by using an IonPac AS12A-SC Analytical Column equipped with an IonPac AG12A-SC Guard Column, 4 mm. Carbonate 1.8 mM/bicarbonate 1.7 mM was employed as the eluent at a flow rate of 2.0 mL/min. The sample loop valve was 10 μL.

The concentration of phosphate in the final enriched RM samples (reported in the *y*-axis of Fig. 1) was also determined to verify that the total content of phosphate (supernatants + final enriched RM) actually corresponded to the phosphate added to RM. The solid phase of RM deriving from each point of the isotherms was dried overnight at 105 °C and digested with 65% HNO_3 + 30% H_2O_2 in a

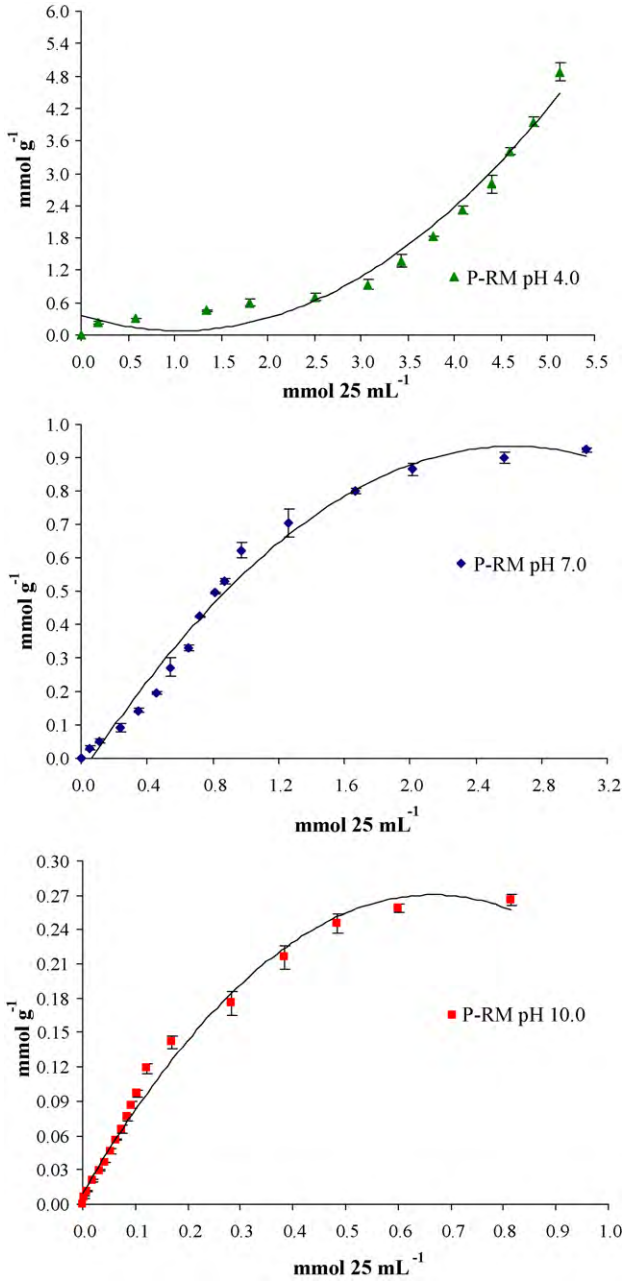

Fig. 1. Adsorption isotherms of phosphate on RM samples at different pH values.

Microwave Milestone MLS 1200. The P concentration was measured by ionic chromatography as described above. The sum of P concentration in the supernatant and in the final enriched RM was not significantly different, at the 95% confidence limit, with respect to the P concentration added to each RM samples. Each experiment was conducted in triplicate and mean values were reported.

2.3. FT-IR spectroscopy

The FT-IR spectra were recorded at room temperature using a Nicolet 380 FT-IR spectrometer equipped with EZ Omnic software. The FT-IR spectra were recorded in the 4000–400 cm^{-1} range, and were collected after 256 scans at 4 cm^{-1} resolution. The KBr disc technique was used for sample preparation. The KBr (FT-IR grade, Fluka) was dried at 200 °C for 24 h. To prepare KBr pellets, 1 mg of RM sample, deriving from the P-RM samples at pH 4.0, 7.0 and 10.0 of the last point of the isotherms, and coming from the extraction procedure steps of P-RM samples at pH 4.0 and 7.0 (see also Section 2.4) was ground 1–2 min together with 200 mg of KBr. The preparation of pellets has been comprehensively described in Castaldi et al. [15].

2.4. Sequential extraction of phosphate from RM samples at pH 4.0, 7.0 and 10.0

The chemical forms of the phosphate bound to the red mud studied were determined using the sequential extraction method proposed by Wenzel et al. [17] with minor modifications. This procedure was adopted in order to better compare the interaction mechanisms that regulate the accumulation and mobility of phosphate and arsenate by the same red mud [15]. Particularly at step 3 we used NaH_2AsO_4 as extracting agent in the place of $NH_4H_2PO_4$. This modification was adopted to extract the phosphate specifically sorbed, given the competition of arsenate for the same adsorption sites in red mud samples.

RM samples (1 g) saturated with phosphate at pH 4.0, 7.0 and 10.0, deriving from the last point of the isotherms, were placed in 50 mL centrifugation tubes and treated with 25 mL of distilled water (pH 6.5) and shaken for 2 h at room temperature to extract the soluble phosphate (Step 0). These samples were then treated with 25 mL of 0.05 M $(NH_4)_2SO_4$ and shaken for 4 h at 20 °C to extract the phosphate non-specifically sorbed (Step 1). The same RM samples were then treated with 25 mL of 1 M NaH_2AsO_4 and shaken for 16 h at 20 °C to extract the phosphate specifically sorbed (Step 2). The higher concentration of the NaH_2AsO_4 used in Step 2 (1 M) with respect to that of $NH_4H_2PO_4$ used in the Wenzel procedure (0.05 M [15]), was adopted to guarantee an excess addition of NaH_2AsO_4. The samples were then treated with 25 mL of 0.2 M NH_4^+-oxalate buffer (pH 3.25) and shaken for 4 h in the dark at 20 °C to extract the phosphate associated with amorphous and poorly crystalline hydrous oxides of Fe and Al (Step 3) and with 25 mL of 0.2 M NH_4^+-oxalate buffer + 0.1 M ascorbic acid (pH 3.25) and shaken for 1/2 h in a water basin at 96 °C (±3) in the light to extract the phosphate associated with well-crystallized hydrous oxides of Fe and Al (Step 4).

After each step of the extraction process the RM samples were centrifuged at 8000 rpm for 10 min and filtered to separate the liquid and solid phases. After the fifth washing, the residual fraction of P was determined by drying the solid phase overnight at 105 °C and digesting it with 65% HNO_3 + 30% H_2O_2 in a Microwave Milestone MLS 1200. The P concentration was measured by ionic chromatography as described above. The sum of P concentration determined in the supernatant after each extraction step and that present in the final enriched RM was not significantly different, at the 95% confidence limit, with respect to the P concentration in RM samples saturated with phosphate. The residual fraction mentioned in the text is that determined after total dissolution of RM.

Each step of the sequential extraction procedure (at the three pH values) was carried out on three samples and the mean values were reported.

3. Result and discussion

3.1. Main features of the sorbent

Table 1 shows the main chemical properties of the RM samples at different pH values used in the study. A detailed discussion of data obtained is reported in a previous manuscript [15]. EDX analyses revealed that the RM_{nt} was rich in O (35.12 wt.%), Fe (30.35 wt.%), Al (9.65 wt.%) and C (9.15 wt.%) (Table 1). A mixture of eight phases was retrieved in the untreated red mud, and the acid-

ification of samples changed the mineralogical composition of this RM. Red mud samples at pH 4.0 showed a loss, proton-promoted, of acid-soluble fractions like boehmite and cancrinite. This dissolution could have contributed to the increase of the XRD-amorphous phase, and the solubilized Al and Si retained in the residue may play an important role in the removal of anions in aqueous solution [18].

3.2. Adsorption isotherms of phosphate on RM at pH 4.0, 7.0 and 10.0

The sorption of phosphate by red mud was studied at pH 4.0, 7.0 and 10.0. The adsorption isotherms obtained at three pH values were different in the shape and in the amount of P sorbed. The adsorption of P by RM at pH 4.0 could be the result of different adsorption steps. In particular when phosphate is present at low concentration (<0.15 M), the sorption could be attributed to a chemical interaction (the first six points of the isotherm) [19]. Subsequently, the isotherm shape indicated that the adsorption process was directly proportional to the concentration of the anion in solution and the isotherm did not reach a defined plateau (P_{ads}/P_{added} ratio increasing) [13]. The second part of the isotherm could be attributed to a slow precipitation of phosphate at the RM surface [20] or to a slow and progressive coagulation due to phosphate that bonded and bridged primary particles [3,21]. By contrast, the sorption isotherms at pH 7.0 and 10.0 were concave to the *x*-axis and a plateau was reached in both curves (Fig. 1). The phosphate sorption by RM at these two pH values decreased as the concentration of P increased, which indicated that the adsorption depended upon the availability of the binding sites for phosphate [13].

The isotherm analyses showed that different concentrations of phosphate were sorbed at different pH values. Particularly the phosphate sorption followed the order: P-RM pH 4.0 (4.871 mmol g^{-1}) > P-RM pH 7.0 (0.924 mmol g^{-1}) > P-RM pH 10.0 (0.266 mmol g^{-1}) (Fig. 1). Significant enhancement of adsorption capacities was achieved at pH 4.0, where the RM adsorption capacity was 5.3 and 18.3 times the amount sorbed into RM at pH 7.0 and 10.0 respectively. These results are in agreement with those reported by other researches in which the authors demonstrated that increasing pH values result in reduced phosphate adsorption on the activated and non treated red mud [2,4,9–10].

Since the anionic sorption is favoured by electrostatic attraction and/or coupled with release of OH^- ions, it should be facilitated by low pH values. Therefore, the lower phosphate sorbed in RM at pH 7.0 and 10.0, with respect to pH 4.0, should be due a higher competition between the anions OH^- and $H_2PO_4^-/HPO_4^{2-}$. Besides, at pH values higher than 4.77 (the pH_{PZC} of red mud) the surface of the RM possesses more negative charges, therefore at pH 7.0 and 10.0 the repulsion of the negatively charged phosphate species in solution should increase, resulting in lower RM adsorption capacity [10,15].

The sorption behaviour of phosphate as a function of the pH was similar to that reported for arsenate on the same RM in our previous manuscript [15], while the quantities of the two anions sorbed were very different. For example, the phosphate sorbed on RM at pH 4.0 was three times higher with respect to arsenate sorbed on RM at the same pH. These differences are not in line with a rather general literature consensus which considers phosphate and arsenate as having similar reactivity and adsorption behaviour on solid surfaces [1,22]. The differences observed in the differential adsorption of arsenate and phosphate by red mud could be tentatively explained by a different ligand-exchange mechanism for the two anions, and/or a different reactivity and precipitation of phosphate and arsenate anions on the surface of red mud [4].

In order to describe the adsorption of phosphate into red mud two types of models, Langmuir and Freundlich isotherms, were applied to describe the equilibrium adsorption of P from liquid solution.

Table 2
The Langmuir and Freundlich parameters relating to the phosphate [P] adsorption into RM samples.

Model	Parameters		
Langmuir isotherm	b (mmol g^{-1})	K (L $mmol^{-1}$)	R^2
P-RM pH 7.0	1.078	0.032	0.97
P-RM pH 10.0	0.240	1.181	0.98
Model	Parameters		
Freundlich isotherm	K_F (mmol g^{-1})	$1/n$	R^2
P-RM pH 7.0	0.654	0.492	0.85
P-RM pH 10.0	0.476	0.566	0.89

The Langmuir equation, which is the simplest and most common model assuming monolayer adsorption, was applied for adsorption equilibrium as follows:

$$\frac{x}{m} = \frac{KbC}{1 + KC};$$

the Langmuir parameter b refers to maximum adsorption capacity and K is a proportional constant of the adsorption energy [9].

The Freundlich model is an empirical equation employed to describe heterogeneous systems [2,10]. The Freundlich isotherm can be expressed as:

$$\frac{x}{m} = K_F C^{1/n}$$

were K_F and n are the Freundlich exponent.

Comparison between isotherms models showed that the Langmuir isotherm represents the adsorption process better than the Freundlich isotherm, in agreement with the results of Li et al. [2]. The higher correlation coefficients (R^2) for Langmuir isotherm in P-RM at pH 7.0 and 10.0 was a clear evidence (Table 2). The low correlation coefficients ($R^2 < 0.50$, values not showed) for Langmuir and Freundlich isotherms in P-RM at pH 4.0 showed that, at this pH value, there were different interaction mechanisms between phosphate and red mud, which could be assigned to chemical adsorption and precipitation of this anion.

The highest adsorption values of phosphate onto RM at pH 7.0 and 10.0, obtained from the Langmuir's equation, agreed with the experimental results (Table 2). The maximum phosphate adsorption b in RM at pH 7.0 was in fact higher than phosphate adsorption b at pH 10.0. These results support the hypothesis previously proposed, hence suggesting that a pH increase decreased the phosphate sorption, but at the same time, as highlighted by the Langmuir's parameter K, this anion formed stronger bonds with the red mud surfaces at pH 10.0 rather than pH 7.0.

The infrared characteristics of red muds saturated with phosphate were studied on P-RM at pH 4.0, 7.0 and 10.0, and compared with RM not exchanged with phosphate at the same pH values (Fig. 2).

In all of the spectra a strong band was present in the hydroxyl stretching region at 3400–3300 cm^{-1}. This was likely due to the presence of H_2O in the red muds [15–16]. A band at 3090 cm^{-1}, which could be ascribed to O–H stretching vibration of crystalline boehmite [23], was also visible in all the spectra. This band was poorly resolved in P-RM at pH 4.0 and 7.0 and the losing of this signal could provide evidence for a P–surface direct bonding with the boehmite phase of red mud.

In all the samples a band at 1630 cm^{-1} was detected. This was attributed to the water molecules occluded inside the aluminosilicate structure [24]. The absorption band of carbonates, which are incorporated in the main channel of cancrinite [25], appeared

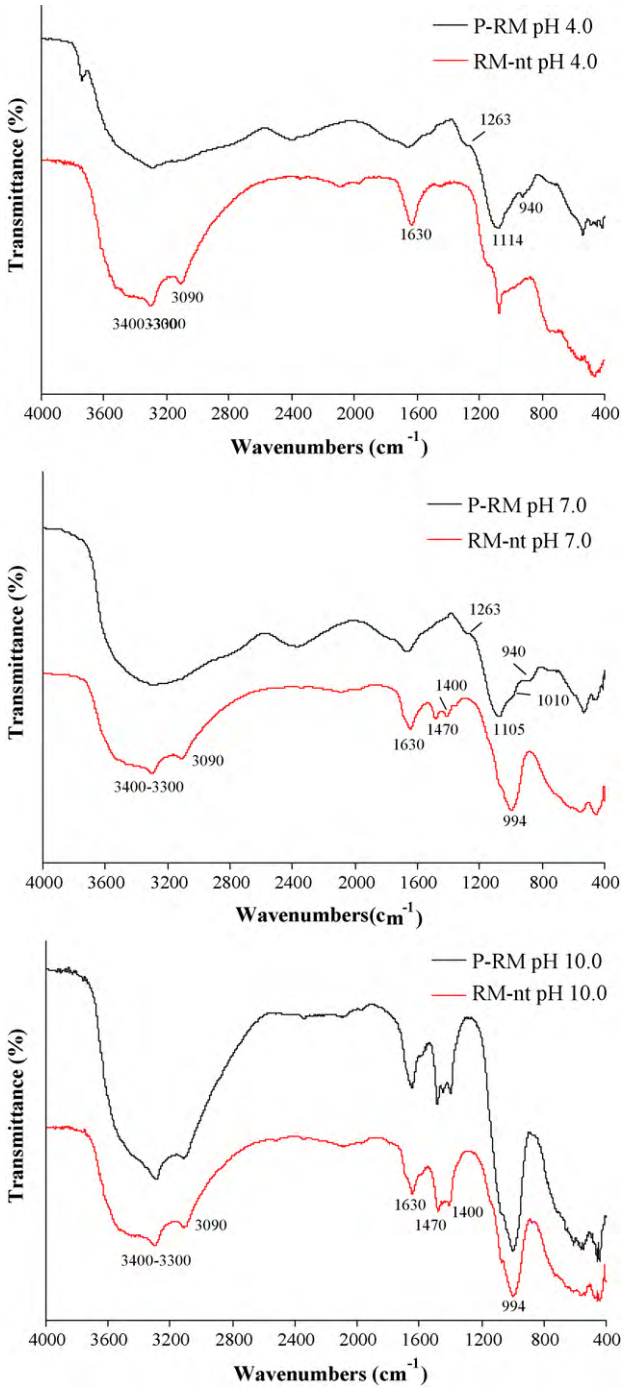

Fig. 2. FT-IR spectra of RM_{nt} and P-RM at different pH values.

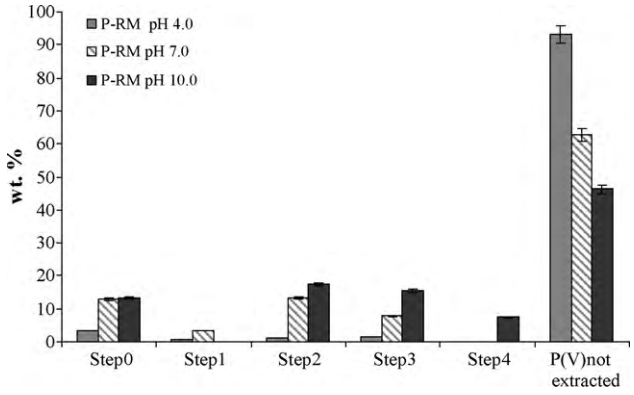

Fig. 3. Percentage of phosphate extracted with H_2O (Step 0); $(NH_4)_2SO_4$ (Step 1); NaH_2AsO_4 (Step 2); NH_4^+-oxalate (Step 3) NH_4^+-oxalate buffer+ascorbic acid (Step 4), and not extracted from P-RM at different pH values.

within the 1410–1470 cm^{-1} region in the samples at pH 7.0 and 10.0. The peak recorded at 1400 cm^{-1} in the samples at pH 7.0 and pH 10.0 could be attributed to NO_3^- present in both cancrinite and sodalite [4]. The band at 994 cm^{-1} observed in samples at pH 7.0 and pH 10.0 could be assigned to the stretching vibrations of Si(Al)–O. This band is sensitive to the content of structural Si and Al [26]. The decreased intensity of this band in RM_{nt} at pH 4.0 was due to the dissolution of cancrinite after the acid treatment, as highlighted by XRD analyses (Table 1).

To evaluate, through the FTIR technique, the interaction mechanisms between the phosphate species and RM, we focused our attention on a part of the midinfrared region, 750–1250 cm^{-1}, where bands associated with various P–O(H) stretching vibrations were found (see also [27–29]). No significant differences were observed in RM spectra between the samples not exchanged and exchanged with phosphate at pH 10.0 with respect to pH 4.0 and 7.0.

The spectra of P-RM at pH 4.0 and 7.0 were dominated by a broad band centred at 1114 and 1105 cm^{-1} respectively. The spectrum of P-RM at pH 7.0 showed the presence of two other shoulders occurring at lower wavenumbers, at approximately 1010, and 940 cm^{-1}. By contrast, in the spectrum of P-RM at pH 4.0, only the shoulder at 940 cm^{-1} was visible. The broad IR bands and the shoulders identified in P-RM at pH 4.0 and 7.0, could be assigned to the P–O(H) stretching ν_3 modes, associated to inner-sphere surface complexes of phosphate on Fe and Al phases of red muds [3,27,29–30]. This broad band may also represent an assemblage of a series of overlapping bands associated with a set of different phosphate surface complexes [31], that probably covered the shoulder at 1010 cm^{-1} in the spectrum of P-RM at pH 4.0. The presence of multiple different phosphate complexes at the red mud surfaces is not unlikely given the complex nature of this substrate, which likely leads to a larger variety in the characteristics of surface sites available for phosphate complexation [30].

The presence of a broad IR band, centred at 1114 and 1105 cm^{-1} in P-RM at pH 4.0 and 7.0 respectively could also indicate the formation of metal-phosphate precipitate on red mud surfaces [28,32]. According to the results reported by Rokita et al. [32], this band could be assigned to the stretching vibrations of PO_4^{3-} tetrahedra, arising from a precipitate of aluminium phosphate. An evidence for this was the presence of a shoulder at 1263 cm^{-1} in P-RM at pH 4.0 and 7.0, which could be assigned to PO_4^{3-} stretching modes of aluminium phosphates [33,34].

However, the FT-IR analysis was unable to distinguish among the type of the complexes formed between the sorbent and phosphate anions, and the metal-phosphate precipitation at the surface of red mud [28]. In this particular case, a balance between the surface precipitation of phosphate phases and a true surface complexation of phosphate ions could be hypothesised.

A comparison of the RM spectra, not treated and exchanged with phosphate at pH 7.0, showed that the most considerable difference, besides the appearance of a new band at 1105 cm^{-1}, was the complete disappearance of the peaks at 1470, 1400 and 994 cm^{-1}, and the substantial reduction of the peak intensity at 1630 cm^{-1} (Fig. 3). Also the comparison of RM_{nt} and P-RM spectra at pH 4.0 showed the disappearance of the peak at 1630 cm^{-1}. All these peaks were directly related to the presence of cancrinite and sodalite phases of RM. Therefore, a partial and/or total ligand-promoted dissolution of tectosilicates at pH 4.0 and 7.0 was very likely.

3.3. Sequential extraction of phosphate from RM samples at pH 4.0, 7.0 and 10.0

To better understand the different interaction mechanisms between the red mud and the phosphate sorbed, samples of red mud saturated with phosphate were treated with solutions of gradually increasing extraction strength [15,17].

The fractions extracted with H_2O, which are the most soluble and bioavailable fractions, were less than 20% of the phosphate adsorbed in RM samples and followed the order P-RM pH 10.0 > P-RM pH 7.0 > P-RM pH 4.0. Particularly, the lowest concentrations of phosphate were detected in RM samples at pH 4.0 extracted with H_2O (Fig. 3). This finding was rather unexpected. A higher concentration of water-soluble phosphate in RM at pH 4.0 with respect to pH 7.0 and 10.0, was originally hypothesized as a consequence of physical interactions between the phosphate and the positive charged surface of RM at this pH value. Probably, in the RM at pH 4.0, phosphate, after an initial electrostatic interaction, formed chemical bonds with functional groups present on the sorbent surface and/or formed precipitates unsoluble in water.

The amount of phosphate extracted with $(NH_4)_2SO_4$, which is indicative of the relatively labile exchangeable fractions, particularly with phosphate bounded through outer-sphere complexes, was very low in all the red mud samples. The amount of phosphate extracted with NaH_2AsO_4, which represents the phosphate specifically sorbed, was higher in RM at pH 10.0 with respect to pH 4.0 and 7.0. Also the amount of phosphate extracted with oxalate and ascorbic acid (Steps 3 and 4), which is indicative of the phosphate fractions associated with amorphous, poorly crystalline and well-crystallized oxides and oxyhydroxides of Fe and Al [17], was higher in P-RM at pH 10.0 with respect to the P-RM at pH 4.0 and 7.0. The residual fractions of P in RM at pH 4.0, 7.0 and 10.0, which would not be expected to be readily released under natural conditions, were respectively 93, 62 and 46 wt.% of the phosphate adsorbed (Fig. 3).

The results of the sequential extraction procedure showed that low quantities of phosphate sorbed in RM at pH 4.0 and 7.0 (<38 wt.%) were in the form of physically and chemically bounded fractions, while the residual fractions of phosphate were more than 60 wt.% in all the doped red mud samples. Probably, at these pH values the main mechanism governing the adsorption process involved the formation of chemical compounds in which the phosphate was incorporated as a structural component of minerals with low-solubility (e.g., calcium iron phosphates or calcium aluminium phosphates). By contrast, a more important sorption mechanism at pH 10.0 was phosphate chemisorption on iron and aluminium phases of RM.

To better understand the interaction between the phosphate and red mud, FT-IR analyses of P-RM at pH 4.0 and 7.0 were performed after each sequential extraction step (Figs. 4 and 5). The band which peaked at 1114 and 1105 cm^{-1} in P-RM at pH 4.0 and 7.0 respectively, was progressively more and more flattened as the extraction steps proceeded. After the extraction with NaH_2AsO_4 (Step 2) a new band at 865 cm^{-1} was evident. The intensity of this band, which increased at decreasing of pH, could be assigned to As–O stretching vibrations of the adsorbed arsenate species [15]. The appearance of a band due to the arsenate sorbed, and the contemporary decrease of intensity of the phosphate band, indicated a partial substitution of phosphate with arsenate, or the availability in P-RM of active binding sites for arsenate.

The band assigned to the phosphate sorption did not disappear after the extraction with NH_4^+-oxalate and ascorbic acid (Step 3 and 4), which quantified the phosphate sorbed into oxides and oxyhydroxides of Fe and Al. Therefore, it was possible to hypothesize that the phosphate sorbed on red muds was mainly bound to phases different from the oxides and oxyhydroxides of Fe and Al

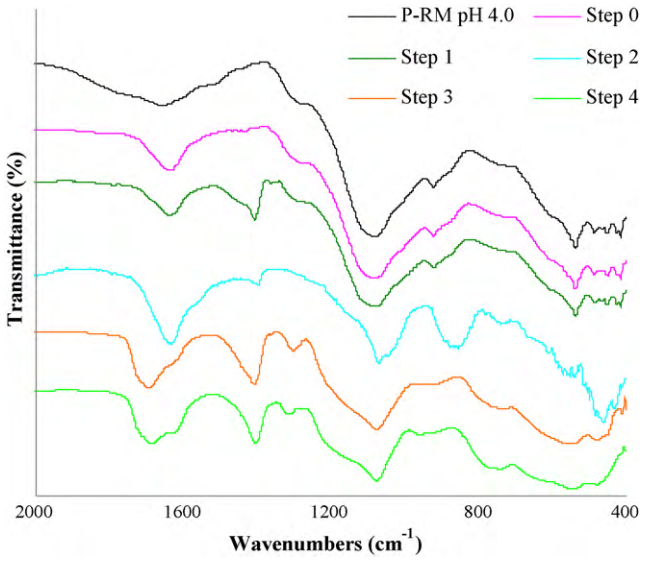

Fig. 4. FT-IR spectra of P-RM at pH 4.0 after the sequential extraction steps.

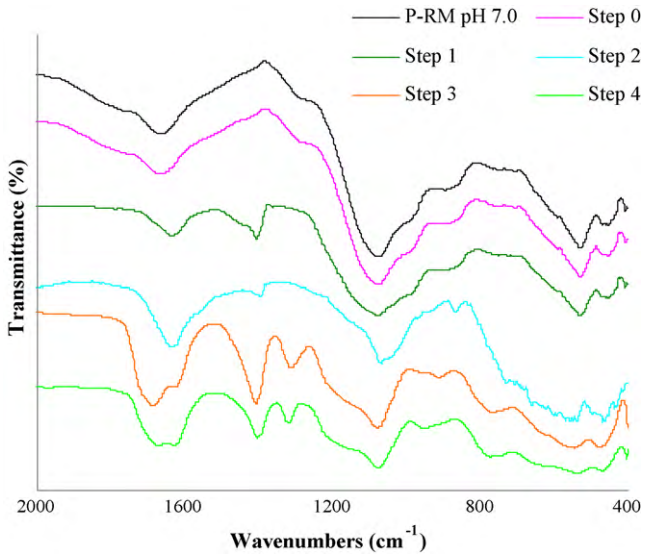

Fig. 5. FT-IR spectra of P-RM at pH 7.0 after the sequential extraction steps.

such as the tectosilicates. Alternatively, the phosphate adsorption process involved the formation of metal phosphate precipitates of low-solubility (e.g., aluminium phosphates).

The spectrum of Step 3 showed new bands at 1320 cm^{-1} (also visible in the Step 4 spectrum) and at 1685 cm^{-1}, which were assigned respectively to C=O stretching vibrations of outer-sphere adsorption of oxalate [35] and to the νC=O stretches originating from the Fe-oxalate formed [36].

4. Conclusions

The red mud used in this study showed a sorption capacity for phosphate that was pH dependent. In particular, the concentrations of phosphate sorbed increased with the pH decrease. Isotherm analyses of arsenate and phosphate on red mud samples, showed a different sorption capacity of the sorbent towards two anions. The phosphate sorbed in RM at pH 4.0 was ~3.0 times higher with respect to arsenate. It can be hypothesized that different interaction mechanisms occurred between phosphate, arsenate and red muds, such as chemical sorption, precipitation and dif-

fusion in the pores and cavities of the framework of red mud phases.

Based on the roles played by phosphate ions during the sorption reactions, it is possible to suggest a coordination-assisted dissolution process for some of the chemical phases of RM at pH 4.0 and 7. Thus, besides a ligand-exchange mechanism, also a metal-phosphate precipitation on RM surfaces could be proposed. This hypothesis was supported by the sequential extraction results that showed the presence of low concentration of phosphate physically and chemically bounded to RM predominantly at pH 4.0.

The FT-IR analyses showed a broad band at 1114 and 1105 cm^{-1} in the spectra of RM exchanged with phosphate at pH 4.0 and 7.0. This band was likely arising from the overlap of different bands, and this could mean the presence of metal-phosphate precipitates, particularly precipitates of aluminium phosphate. In addition, FT-IR spectroscopy showed that the phases probably subject to ligand-promoted dissolution in RM at pH 4.0 and 7.0 were sodalite and cancrinite.

The results obtained showed that the adsorbing properties of red mud studied are related to their capacity to decrease the mobility of the phosphate through exchange and precipitation reactions. In addition, the results obtained suggest the need for further studies that would take into account the interaction between red mud and phosphate and arsenate when these latter are simultaneously present, in order to better clarify the affinity and competition of two anions towards the red mud.

References

[1] J. Antelo, M. Avena, S. Fiol, R. López, F. Arce, Effects of pH and ionic strength on the adsorption of phosphate and arsenate at the goethite–water interface, J. Colloid Interface Sci. 285 (2005) 476–486.

[2] Y. Li, C. Liu, Z. Luan, X. Peng, C. Zhu, Z. Chen, Z. Zhang, J. Fan, Z. Jia, Phosphate removal from aqueous solutions using raw and activated red mud and fly ash, J. Hazard. Mater. 137 (2006) 374–383.

[3] C. Luengo, M. Brigante, J. Antelo, M. Avena, Kinetic of phosfate adsorption on goethite:comparing batch adsorption and ATR-IR measuraments, J. Colloid Interface Sci. 300 (2006) 511–518.

[4] Y. Zhao, J. Wang, Z. Luan, X. Peng, Z. Liang, L. Shi, Removal of phosphate from aqueous solution by red mud using a factorial design, J. Hazard. Mater. 165 (2009) 1193–1199.

[5] S. Deiana, A. Palma, A. Premoli, C. Senette, Possible role of the polyuronic components in accumulation and mobilization of iron and phosphate at the soil–root interface, Plant Physiol. Biochem. 45 (2007) 341–349.

[6] G. Zhang, H. Liu, R. Liu, J. Qu, Removal of phosphate from water by a Fe–Mn binary oxide adsorbent, J. Colloid Interface Sci. 335 (2009) 168–174.

[7] J. Chen, H. Kong, D. Wu, Z. Hu, Z. Wang, Y. Wang, Removal of phosphate from aqueous solution by zeolite synthesized from fly ash, J. Colloid Interface Sci. 300 (2006) 491–497.

[8] M.W. Kamiyango, W.R.L. Masamba, S.M.I. Sajidu, E. Fabiano, Phosphate removal from aqueous solutions using kaolinite obtained from Linthipe, Malawi, Phys. Chem. Earth 34 (2009) 850–856.

[9] J. Pradhan, J. Das, S. Das, R. Singh Thakur, Adsorption of phosphate from aqueous solution using activated red mud, J. Colloid Interface Sci. 204 (1998) 169–172.

[10] W. Huang, S. Wang, Z. Zhu, L. Li, X. Yao, V. Rudolph, F. Haghseresht, Phosphate removal from wastewater using red mud, J. Hazard. Mater. 158 (2008) 35–42.

[11] C. Liu, Y. Li, Z.K. Luan, Z.Y. Chen, Z. Zhang, Z. Jia, Adsorption removal of phosphate from aqueous solution by active red mud, J. Environ. Sci. 19 (2007) 1166–1170.

[12] H. Genç, J.C. Tjell, D. McConchie, O. Schuiling, Adsorption of arsenate from water using neutralized red mud, J. Colloid Interface Sci. 264 (2003) 327–334.

[13] L. Santona, P. Castaldi, P. Melis, Evaluation of the interaction mechanisms between red muds and heavy metals, J. Hazard. Mater. 136 (2006) 324–329.

[14] G. Garau, P. Castaldi, L. Santona, P. Deiana, P. Melis, Influence of red mud, zeolite and lime on heavy metal immobilization, culturable heterotrophic microbial populations and enzyme activities in a contaminated soil, Geoderma 142 (2007) 47–57.

[15] P Castaldi, M. Silvetti, S. Enzo, P. Melis, Study of sorption processes and FT-IR analysis of arsenate sorbed onto red muds (a bauxite ore processing waste), J. Hazard. Mater. 175 (2010) 172–178.

[16] P. Castaldi, M. Silvetti, L. Santona, S. Enzo, P. Melis, XRD, FT-IR, and thermal analysis of bauxite ore-processing waste (red mud) exchanged with heavy metals, Clay, Clay Miner. 56 (2008) 461–469.

[17] W.W. Wenzel, N. Kirchbaumer, T. Prohaska, G. Stingeder, E. Lombi, D.C. Adriano, Arsenic fractionation in soils using an improved sequential extraction procedure, Anal. Chim. Acta 436 (2001) 309–323.

[18] B. Koumanova, M. Drame, M. Popangelova, Phosphate removal from aqueous solution using red mud wasted in bauxite Bayer's process, Resour. Conserv. Recy. 19 (1997) 11–20.

[19] N.C. Brandy, R.R. Weil, Soil colloids: their nature and practical significance, in: N.C. Brandy, R.R. Weil (Eds.), The Nature and Properties of Soils, 13th ed., Prentice Hall, New Yersey, 2002, pp. 147–187.

[20] R. Martin, R. Smart, K. Tazaki, Direct observation of phosphate precipitation in the goethite/phosphate system, Soil Sci. Soc. Am. J. 52 (1988) 1492–1500.

[21] M.A. Anderson, M.I. Tejedor-Tejedor, R.R. Stanforth, Influence of aggregation on the uptake kinetics of phosphate by goethite, Environ. Sci. Technol. 19 (1985) 632–637.

[22] Y. Gao, A. Mucci, Acid base reactions, phosphate and arsenate complexation, and their competitive adsorption at the surface of goethite in 0.7 M NaCl solution, Geochim. Cosmochim. Acta 65 (2001) 2361–2378.

[23] A. Boumaza, L. Favaro, J. Lédion, G. Sattonnay, J.B. Brubach, P. Berthet, A.M. Huntz, P. Roy, R. Tétot, Transition alumina phases induced by heat treatment of boehmite: an X-ray diffraction and infrared spectroscopy study, J. Solid State Chem. 182 (2009) 1171–1176.

[24] A. Gök, M. Omastová, J. Prokeš, Synthesis and characterization of red mud/polyaniline composites: electrical properties and thermal stability, Eur. Polym. J. 43 (2007) 2471–2480.

[25] J. Mon, Y. Deng, M. Flury, J.B. Harsh, Cesium incorporation and diffusion in cancrinite, sodalite, zeolite and allophone, Micropor. Mesopor. Mater. 86 (2005) 277–286.

[26] M. Majdan, M. Kowalska-Ternes, S. Pikus, P. Staszczuk, H. Skrzypek, E. Zixęba, Vibrational and scanning electron microscopy study of the mordenite modified by Mn, Co, Ni, Cu, Zn and Cd, J. Mol. Struct. 649 (2003) 279–285.

[27] M.I. Tejedor-Tejedor, M.A. Anderson, The protonation of phosphate on the surface of goethite as studied by CIR-FTIR and electrophoretic mobility, Langmuir 6 (1990) 602–611.

[28] P. Persson, N. Nilsson, S. Sjöberg, Structure and bonding of orthophosphate ions at the iron oxide–aqueous interface, J. Colloid Interface Sci. 177 (1996) 263–275.

[29] Y. Arai, D.L. Sparks, ATR-FTIR spectroscopic investigation on phosphate adsorption mechanisms at the ferrihidrite-water interface, J. Colloid Interface Sci. 241 (2001) 317–326.

[30] E.J. Elzinga, D.L. Sparks, Phosphate adsorption onto hematite: an in situ ATR-FTIR investigation of the effects of pH and loading level on the mode of phosphate surface complexation, J. Colloid Interface Sci. 308 (2007) 53–70.

[31] R.L. Parfitt, R.J. Atkinson, R.S. Smart, The mechanism of phosphate fixation by iron oxides, Soil Sci. Am. Proc. 39 (1975) 837–841.

[32] M. Rokita, M. Handke, W. Mozgawa, The $AlPO_4$ polymorphs structure in the light of Raman and IR spectroscopy studies, J. Mol. Struct. 555 (2000) 351–356.

[33] V.C. Farmer, The infrared spectra of minerals. Mineralogical Society Monograph 4, 1974, London.

[34] S.C. Pînzaru, B.P. Onac, Raman study of natural berlinite from a geological phosphate deposit, Vib. Spectrosc. 49 (2009) 97–100.

[35] S.J. Hug, D. Bahnemann, Infrared spectra of oxalate, malonate and succinate adsorbed on the aqueous surface of rutile, anatase and lepidocrocite measured with in situ ATR-FTIR, J. Electron Spectrosc. 150 (2006) 208–219.

[36] A. Nevin, J.L. Melia, I. Osticioli, G. Gautier, M.P. Colombini, The identification of copper oxalates in a 16th century Cypriot exterior wall painting using micro FTIR, micro Raman spectroscopy and gas chromatography–mass spectrometry, J. Cult. Herit. 9 (2008) 154–161.